J Mater Sci: Mater Med (2009) 20:2395–2400
DOI 10.1007/s10856-009-3813-2

Synthesis and characterization of biocomposites with different hydroxyapatite–collagen ratios

Lidia A. Sena · Mirta M. Caraballo · Alexandre M. Rossi · Gloria A. Soares

Received: 25 January 2009 / Accepted: 25 June 2009 / Published online: 8 July 2009

Abstract Hydroxyapatite (HA)-type I collagen (Col) composite is a tissue-engineered bone graft which can act as a carrier or a template structure for cells or any other agents. In this paper, the effect of Col ratio on the scaffold structure and composition was analyzed. Scaffolds composed by HA/Col with different weight ratios (80:20; 50:50; 20:80, and 10:90) were produced by the precipitation method at pH 8–9, 37°C and 6 h of ripening. Using X-ray diffraction data, the Rietveld structure refinement showed that the size of HA crystals along the c-axis direction (002) decreases significantly in the presence of Col. Thus, the HA crystal shape turned from needle-like in pure HA, into spherical, in the 10:90 composite due to Col fibrillogenesis. The homogeneity of the composite was significantly dependent on the amount of Col in it. HA/Col 20/80 composite presented HA particles in a more homogenous way. Such a biocomposite was successfully produced in a rapid way and it is potentially useful for both small tissue repairs and engineering.

L. A. Sena (✉)
Materials Metrology Division, Inmetro,
Duque de Caxias, RJ, Brazil
e-mail: lidiasena@pq.cnpq.br

L. A. Sena · G. A. Soares
Metallurgical and Materials Engineering Department,
Federal University of Rio de Janeiro,
Rio de Janeiro, RJ, Brazil

M. M. Caraballo
Department of Exact Sciences, Alfenas Federal University,
Alfenas, MG, Brazil

A. M. Rossi
Brazilian Center for Physics Research (CBPF), Rio de Janeiro,
RJ, Brazil

1 Introduction

A bone is a complex, highly-organized, mineralized tissue, which is constantly being remodeled. Yet, an imbalance in this process may lead to reduced skeletal bone mass. Thus, it is necessary to either restore or to replace the function of the traumatized or degenerated bone tissue [1]. The current progress in biomineralization research allows the development of biomimetic materials in accordance with the biological principles [2].

The development of materials for bone reconstruction applications, such as bone graft substitutes, has been strongly affected by both the advent and consolidation of tissue engineering. Third-generation biomaterials are developed focusing on tissue regeneration so as to promote specific cellular responses at a molecular level, with minimally invasive surgery [3]. In the bone substitution process, new tissues are raised and generated in the laboratory through the combination of synthetic or natural scaffolds, cells, and active substances such as morphogenetic proteins and growth factors. Such a process optimizes and accelerates the growth of the surrounding tissue.

A certain number of factors must be taken into consideration when designing a scaffold: (1) The material should have mechanical properties, consistent with the anatomical site into which it is to be implanted; (2) A high surface area is necessary to facilitate cell seeding and diffusion throughout the cells and nutrients structure; (3) Degradation should occur in a ratio that coincides with both the tissue formation rate and the structural integrity within the body. The development of biomimetic scaffolds is being studied by several research groups [4–9]. To develop a scaffold for bone defects filling, some research must be based on bone tissue structure and composition configuration [10–12]. The hydroxyapatite (HA) and collagen (Col) biocomposites

have been examined because of their potential use as bone substitutes [13–15].

However, the natural process of mineralization is still not completely understood [16]. For some authors it begins in vesicles among the Col fibers; then, in the gap areas where the tropocollagen molecules are found [17, 18]. Other research hypothesizes that the beginning of mineralization occurs directly within the gap areas, preferably throughout the axis of the Col fibrils [19, 20]. The accurate preferential orientation of such crystals is still controversial. According to Cool et al. [20], only 25% of the mineral phase is located inside the Col fibril and the remaining 75% would occur outside the Col molecule gap areas, without any apparent preferential orientation. These diverse theories would require the use of different experimental methodologies and characterizations. In addition, bone morphology is highly variable when related to place, age functioning, etc., which hinders its mimetization [21].

A challenge many scientists have attempted to simulate over the past decades is the reproduction of this hierarchical assembly. Currently, the most promising HA/Col composite preparation methodology was proposed by Kikuchi et al. [13]. The main advantages of such a method are the production of controlled orientation of Col fibers and the nucleation of HA crystals along the direction of Col fibrils with a structure similar to the natural bone.

The present paper aims at analyzing the effect of Col ratio on HA/Col scaffold structure and composition. The Col ratio added to the reaction medium was carried out in order to optimize the dispersion of HA crystals within the composite as well as to obtain a homogeneous sample. Scaffolds with HA/Col weight ratios of 80:20; 50:50; 20:80, and 10:90 were produced via precipitation method.

2 Experimental procedure

HA/Col composites with HA:Col weight ratios of 80:20; 50:50; 20:80, and 10:90 were produced by the aqueous precipitation method, using a native Type I Col gel. The preferred methodology was the one proposed by Kikuchi et al. [13]. Collagen solutions containing $Ca(OH)_2$ (99.6 mM) and H_3PO_4 (59.6 mM) were used under the control of pH (pH 8–9), temperature (37°C) and ripening time (6 h). After aging the precipitates for 6 h, the materials were filtered and then lyophilized. In order to maintain the Col fibers intact, part of the composite was dried at a critical point. The effect of the Col fibrillogenesis during the calcium phosphate precipitation was also compared with the production of pure HA under similar conditions.

The experimental materials were then characterized by the use of scanning electron microscopy (SEM, Zeiss DMS 940A) for morphologic evaluation. The samples, mounted on aluminum stubs using double-sided carbon tape, were sputter-coated with a thin layer of gold to avoid electrical charging, and observed after the application of 15 kV of accelerating voltage. The composites and HA powder spectra were analyzed by using the Fourier Transform Infrared Spectroscopy (FTIR, Spectra Tech). The chemical groups were then classified into inorganic and organic phases. The presence of impurities such as amorphous calcium phosphate precursors was also evaluated. After that, the data were recorded in a 4000–400 cm^{-1} spectral range with a 4 cm^{-1} resolution.

X-ray diffraction (XRD, Rigaku Rota Flex) was used to characterize the crystalline phase. XRD measurements were processed in a powder diffractometer, operating with Cu Kα radiation (1.5418 Å), 30 kV, 15 mA, and equipped with graphite monochromator. In order to analyze diffraction patterns precisely, the structural refinement of the HA powder and HA/Col composites diffractograms was carried out so as to determine their crystal size. Based on the XRD results, crystal size was determined by the Rietveld method. The diffractograms were obtained in an angular range of $2\theta = 0$–$100°$, with a step of 0.02°; afterwards, at the rate of 5 s/step. Initially, the phase identification was performed by comparison with the JCPDS data cards.

The Foolproof program was used to implement the Rietveld method. A LaB6 (Aldrich, particles <10 μm) sample was used as an external, standard material for determining not only the zero shift but also the instrumental profile under exactly the same conditions of the step scanning mode performed on the investigated samples. The function of the instrumental resolution was obtained by refining the U, V, W, X, and Y parameters of the diffractogram pattern. Anisotropic analysis of the HA powder and composites diffractograms was performed. In other words, IsizeModel $= -1$, and preferential direction (001) were used when domains were assumed to be in the form of needles. Scale parameters, background, zero, factors regarding size and micro deformation (Y and U), cell parameters (a, b, c, and γ), GauSize, and LorSize were refined.

Some samples were additionally examined by transmission electron microscopy (TEM, JEOL 2000FX) in order to investigate the morphology of HA and other features. For TEM analysis, HA powder was dispersed with ultrasonic vibration in ethanol and deposited on a TEM copper grid, coated with carbon film. HA/Col 80/20 and HA/Col 50/50 composites were fixed with 2.5% glutaraldehyde and washed 3 times at room temperature with a 0.1 M sodium cacodylate buffer. Next, the sample was post-fixed for 1 h in 1% osmium tetroxide in 0.1 M sodium cacodylate buffer, washed again twice with 0.1 M sodium cacodylate buffer, and then dehydrated by the use of a series of ethanol/distilled water solutions. Finally, the samples were embedded

in epoxy resin and prepared using ultramicrotomy (RMC XT 6000-XL).

3 Results and discussion

Figure 1 shows the SEM micrographs obtained for the composites. It is possible to observe a large amount of calcium phosphate (CaP) precipitate on the HA/Col 80/20 composite fibers (Fig. 1a). A significant amount of CaP was poorly adhering to the Col surface and became loose while manipulating the composites. The possibility of particles detachment may cause significant problems concerning cell apoptosis when appraised in vitro and/or in vivo. The same problems were observed in the literature, that is, free particles can migrate into the scaffold that is being formed. A systemic inflammatory response can be generated if the body can neither expel nor dissolve such detached particles [22].

As for the HA/Col 50/50 composite (Fig. 1b), apatite seems to be more strongly attached, and no particle detachment was observed during the manipulation process. The apatite crystals are homogenously distributed within the Col fibers in the 20/80 HA/Col composite (Fig. 1c). However, in the 10/90 HA/Col composite, the high concentration of Col hinders the dispersion of the fibers during their formation, causing an agglomeration of particles linked with native Col fibers (Fig. 1d). A reduced HA crystal–Col fibers interaction can be attributed to a larger and faster fiber agglomeration due to a large amount of raised Col. As a result, only part of the HA grown crystals interacted effectively with the Col fibers.

The FTIR bands assigned to HA powder and HA/Col composites (80/20, 50/50, 20/80, and 10/90 weight ratio) are presented in Table 1. Previous investigations of HA/Col composites preparations have suggested that negatively charged carboxylate groups are responsible for any kind of HA nucleation because of the calcium ions interaction [13]. Comparing the results obtained by other researchers [3, 4], FTIR analysis did not indicate any alterations in the Col vibration mode for none of the used HA–-Col ratios. The spectra of the composites (not shown) presented characteristic bands of a protein, around 1600–1700 cm^{-1}. This evidences carbonyl stretching at 1560 cm^{-1} and it is associated with amide II vibrations in the plan of the N–H and

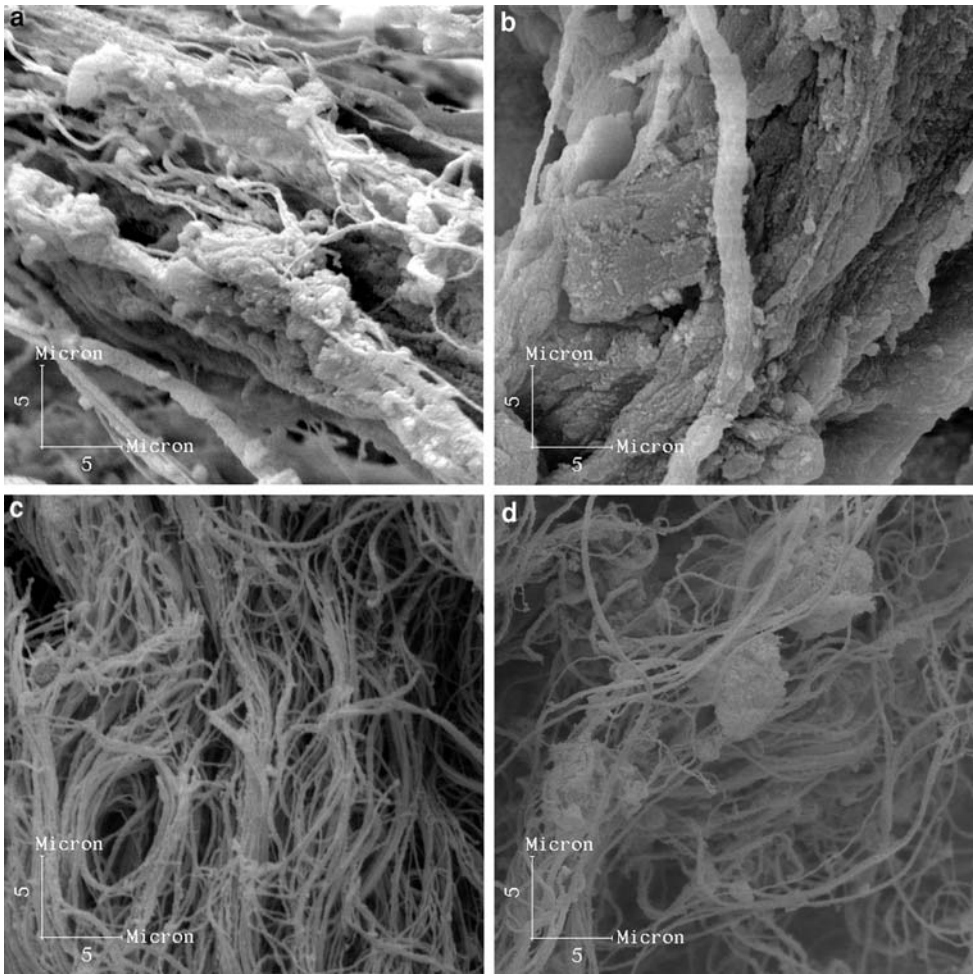

Fig. 1 The SEM micrographs of (**a**) 80:20; (**b**) 50:50; (**c**) 20:80 and (**d**) 10:90 HA:Col weight ratio composites

Table 1 Assignments of the observed vibrational frequencies of HAP and Collagen

Assignments	Observed vibrational frequencies wavenumber (cm^{-1})				
	HA	HA/Col 80/20	HA/Col 50/50	HA/Col 20/80	HA/Col 10/90
Structural OH	3571	–	–	–	–
H_2O adsorbed, N–H (A Amide)	3360	3390	3321	3341	3334
C–H (B Amide)	–	3075	3085	3089	3080
C–H3 group	–	2958	2961	2978	2959
H_2O adsorbed v_2, C=O (I Amide)	1653	1689	1670	1681	1686
N–H (II Amida), C–N	–	1565	1560	1563	1559
CO_3^{2-} v_3, pyrrolidine rings	1452	1457	1446	1456	1459
CO_3^{2-} group v_3	1425	–	–	–	–
$-COO^-$	–	1340	1341	1339	1341
C–N (III Amide), N–H (I Amide)	–	1247	1240	1243	1247
PO_4^{3-}	1172	1165	1140	1110	1159
PO_4^{3-} bend v_3	1088	1088	1080	1081	1082
PO_4^{3-} bend v_3	1025	1018	1017	1017	–
PO_4 stretch v_1	963	960	960	960	–
CO^{3-} group, HPO_4^{2-}	873	873	871	872	–
Structural OH ~630	[a]	[a]	[a]		
PO_4 bend v_4 ~600	[a]	[a]	[a]	[a]	[a]
PO_4 bend v_4 ~570	[a]	[a]	[a]	[a]	[a]

[a] Region with intense noise and low resolution

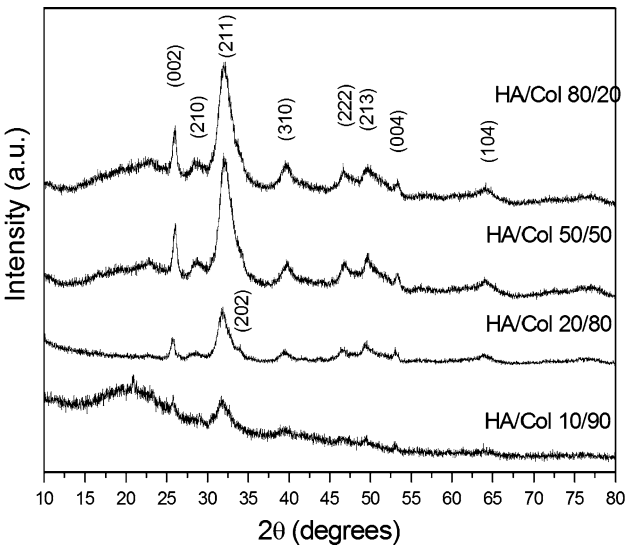

Fig. 2 XRD patterns of the composites HA/Col 80/20, HA/Col 50/50, HA/Col 20/80 and HA/Col 10/90

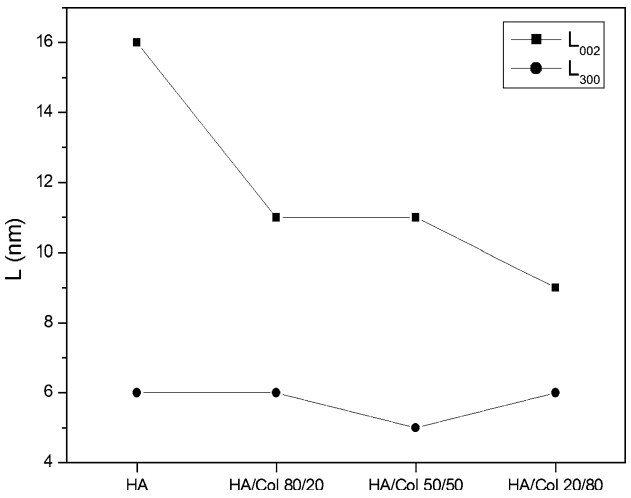

Fig. 3 The crystal sizes in (002) and (300) planes for HA and HA present in the composites HA/Col 80/20, HA/Col 50/50 and HA/Col 20/80

C–H stretch connection. 1450 cm^{-1} indicates the presence of proline and hydroxyproline pyrrolidine rings. The band close to 3400 cm^{-1} is due to O–H stretching. Although some intense vibration mode variations were detected, the values obtained were in agreement with the literature [10]. HA bands are not evident either because of superimposed Col bands or low crystallinity in the formed crystals.

The FTIR bands attributed to HA powder (Table 1) show bands around 3571 cm^{-1} which are generally assigned to the presence of the structural O–H mode stretching. Bands at 1172, 1088, 1025, and 963 cm^{-1} indicate the presence of PO_4^{3-} groups, typically described in the literature [23, 24]. The presence of a wide band—around 3360 cm^{-1}—and another one of 1653 cm^{-1} average intensity indicates the presence of adsorbed water. The presence of a band at

873 cm^{-1} and two bands at 1425 and 1452 cm^{-1} shows that there is a $(CO_3)^{2-}$ group substituting for PO_4^{3-} sites. This is characteristic of the type B carbonated HA. The presence of a band at 873 cm^{-1} can be attributed to HPO_4^{2-} group′s presence. The P–OH connection stretching suggests the formation of a HA deficient in calcium [23]. According to Tadic et al. [24], information on material crystallinity can be observed in the infrared spectrum by looking for bands located between the 590–610 cm^{-1} and 1000 cm^{-1} regions. The HA obtained had wide and insufficiently defined bands in these regions, evidencing low crystallinity. Similar results were verified in the spectra of the composites, which characterized the inorganic constituents.

The XRD patterns of the composites (Fig. 2) revealed a crystalline structure, quite similar to the one of natural bone [25]. Their patterns show several characteristic peaks of HA, which are in very good agreement with the JCPDS card No. 9-432. According to the XRD data refinement results (Fig. 3), in the presence of Col, the size of HA crystal suddenly decreased. However, this effect was basically restricted to one single direction (002 plane). When the HA crystal turns from needle-like (pure HA) into spheroidized crystal (HA–Col composite), HA precipitation is strongly affected by the presence of Col molecules. One of the theories is that Col fibrillogenesis obstructs crystal growth.

It is well known that the presence of some organic substances in the precipitation medium reduces the dielectric constant of the solution [26]. Some proteins are reported to be adsorbed by HA crystals due to their high affinity, causing low crystallinity [27]. According to Veis [28], the matrix-mediated mineralization takes place when compartments and spaces are defined and restricted. The

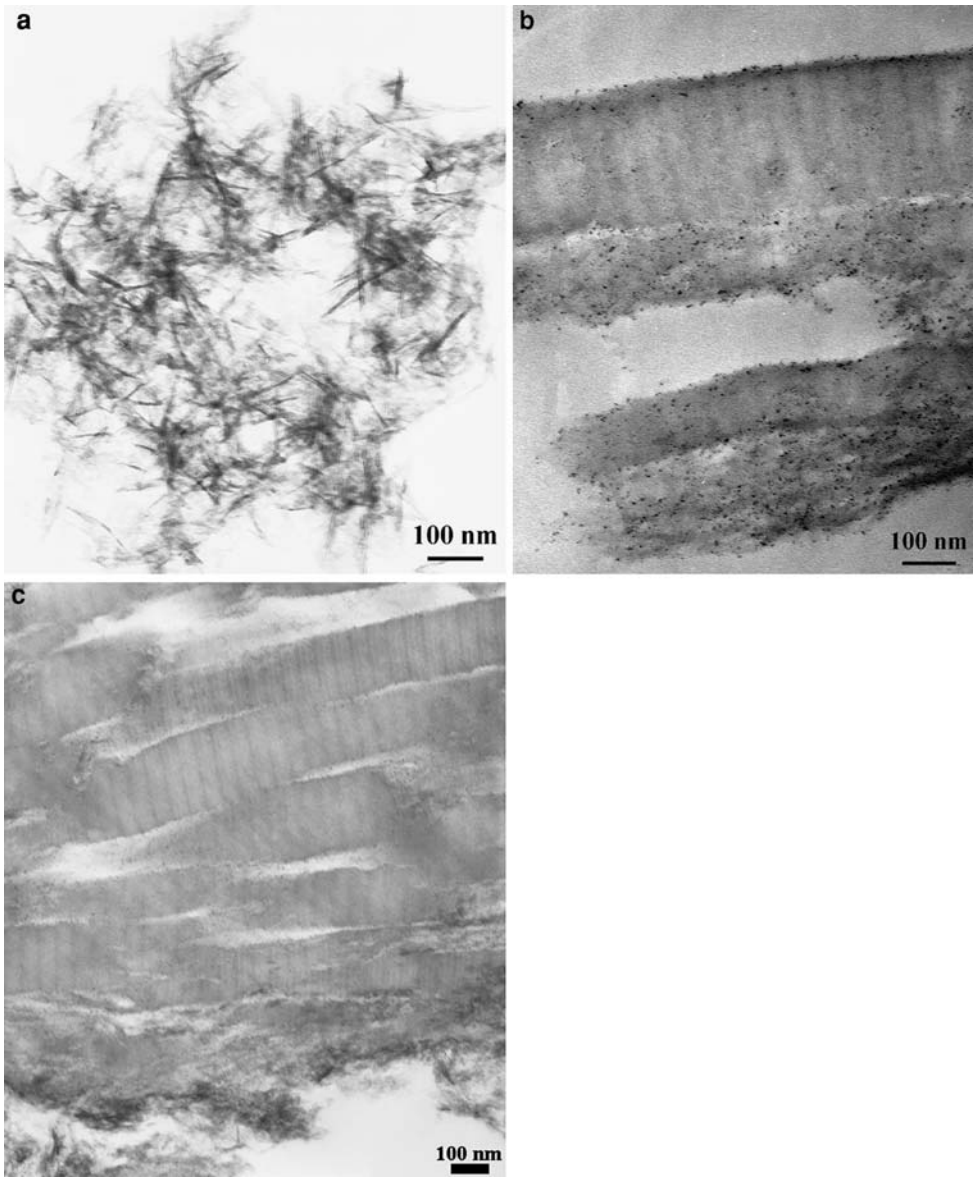

Fig. 4 TEM micrographs of the HA powder (**a**), the Hap/Col biocomposites HA/Col 80/20 (**b**) and HA/Col 50/50 (**c**)

physical size and shape of the spaces may limit a crystal's volume and shape. Even so, there is not enough space to contain all the mineral phases in the gaps. Crystals are distributed throughout Col fibril spaces, which provide stiffness and strength to the composite.

The TEM micrographs confirmed the XRD result. Needle-like crystals of HA, synthesized without Col, can be observed in Fig. 4a. Figure 4b and c shows small, rounded particles, precipitated along the Col fibrils. A typical banding pattern of fibril structure, with a 67 nm (D-periodic) periodicity and a large quantity of crystals formed out of fibrils is also present. In a mature bone, mineral phase can be located in the following three positions: (1) the periodic gap spaces and related channels (intrafibrillar); (2) the pores between microfibrils (intrafibrillar); and (3) the spaces between packed fibrils [27]. Other characterization techniques are being conducted to determine a deeper analysis of this mineral array in the biocomposites. Further in vitro and in vivo studies are also required to confirm the ability to produce composites so as to support bone formation.

4 Conclusions

In the current study, a HA–Col biocomposite scaffold was successfully produced by the precipitation method in a rapid way. The structural characteristics of the Col molecules were preserved during the experiments. Nano-sized HA crystals were tightly deposited along the Col framework during the Col fibril reassembling. Both the morphology and size of the HA crystals were strongly affected by the Col ratio in the synthesis medium. HA crystals decreased in size along the c-axis in the presence of Col, turning from needle-like into spherical shape. The interaction between HA crystals and Col fibers was affected by Col fibrillogenesis. HA/Col 20/80 composite presented HA particles dispersed in a more homogeneous way.

Acknowledgements The authors thank Dr. Virginia C. A. Martins for providing collagen as well as and helpful suggestions. This work was supported by renowned Brazilian agencies such as CNPq, CAPES and FAPERJ.

References

1. Meyer U, Wiesmann HP, Meyer T. Bone and cartilage engineering. New York: Springer; 2006.
2. Green D, Walsh D, Mann S, Oreffo ROC. The potential of biomimesis in bone tissue engineering: lessons from the design and synthesis of invertebrate skeletons. Bone. 2002;30:810–5.
3. Hench LL, Polak JM. Third-generation biomedical materials. Science. 2002;295:1009–14.
4. Ito Y. Tissue engineering by immobilized growth factors. Mater Sci Eng C. 1998;6:267–74.
5. Hutmacher DW. Scaffolds in tissue engineering bone and cartilage. Biomaterials. 2000;21:2529–43.
6. Mcdonough WG, Amis EJ, Kohn J. Critical issues in the characterization of polymers for medical applications. NISTIR-6535, Gaithersburg, MD: U.S. Dept. of Commerce, Technology Administration, National Institute of Standards and Technology; 2000.
7. Sachlos E, Czernuszka JT. Making tissue engineering scaffolds work. Review on the application of solid freeform fabrication technology to the production of tissue engineering scaffolds. Eur Cells Mater. 2003;5:29–40.
8. Wang X, Grogan SP, Rieser F, Winkelmann V, Maquet V, La Berge M, et al. Tissue engineering of biphasic cartilage constructs using various biodegradable scaffolds: an in vitro study. Biomaterials. 2004;25:3681–8.
9. Xu HHK, Simon CG Jr. Self-hardening calcium phosphate composite scaffold for bone tissue engineering. J Orthop Res. 2004;22:535–43.
10. Goissis G, Maginador SVS, Martins VCA. Biomimetic mineralization of charged collagen matrices: in vitro and in vivo study. Artif Org. 2003;27(5):437–43.
11. Lawson AC, Czernuszka JT. Collagen-calcium phosphate composites. Proc Inst Mech Eng Part H J Eng Med. 1998;212(6):413–25.
12. Kobayashi N, Onuma K, Oyane A, Yamazaki A. The role of phosvitin for nucleation of calcium phosphate on collagen. Key Eng Mater. 2004;255:537–40.
13. Kikuchi M, Suetsugu Y, Tanaka J, Itoh S, Ichinose S, Shinomiya K, et al. The biomimetic synthesis and biocompatibility of self-organized hydroxyapatite/collagen composites. Key Eng Mater. 1999;164–165:393–6.
14. Wahl DA, Czernuszka JT. Collagen-hydroxyapatite composites for hard tissue repair. Eur Cells Mater. 2006;11:43–56.
15. Sena LA, Serricella P, Borojevic R, Rossi AM, Soares GA. Synthesis and characterization of hydroxyapatite on collagen gel. Key Eng Mater. 2004;254–256:493–6.
16. Cui FZ, YJ Ge. Self-assembly of mineralized collagen composites. Mater Sci Eng R. 2007;57(1–6):1–2.
17. Lowenstam HA, Weiner S. On biomineralization. Oxford: Oxford University Press; 1989. p. 144–67. (Chap. 9).
18. Landis JL, Silver FH. The structure and function of normally mineralizing avian tendons. Comp Biochem Phys A. 2002;133:1135–57.
19. Weiner S, Traub W. Crystal size and organization in bone. Connect Tissue Res. 1989;21:259–65.
20. Zhang W, Liao SS, Cui FZ. Hierarchical self-assembly of nanofibrils in mineralized collagen. Chem Mater. 2003;15:3221–6.
21. Cool SM, Forwood MR, Campbell P, Bennett MB. Comparisons between bone and cementum compositions and the possible basis for their layered appearances. Bone. 2002;30(2):386–92.
22. Hsu FY, Chueh S-C, Wang YJ. Microspheres of hydroxyapatite/reconstituted collagen as supports for osteoblast cell growth. Biomaterials. 1999;20:1931–6.
23. Legeros RZ. Biological and synthetic apatites. In: Brown PW, Constantz B, editors. Hydroxyapatite and related materials. Boca Raton: CRC Press; 1994. p. 3–28.
24. Tadic D, Peters F, Epple M. Continuous synthesis of amorphous carbonated apatites. Biomaterials. 2002;23:2553–9.
25. Danilchenko SN, Moseke C, Sukhodub LF, Sulkio-Cleff B. X-ray diffraction studies of bone apatite under acid demineralization. Cryst Res Technol. 2004;39:71.
26. Robinson C. Self-oriented assembly of nano-apatite particles: a subunit mechanism for building biological mineral crystals. J Dent Res. 2007;86(8):677–9.
27. Matsumoto T, Okazaki M, Inoue M, Hamada Y, Taira M, Takahashi J. Crystallinity and solubility characteristics of hydroxyapatite adsorbed amino acid. Biomaterials. 2002;23(10):2241–7.
28. Veis A. Mineralization in organic matrix frameworks. Rev Mineral Geochem. 2003;54(1):249–89.